Large Magnetoresistance of Nickel-Silicide Nanowires: Non-Equilibrium Heating of Magnetically-Coupled Dangling Bonds

T. Kim,[†,‡] R. V. Chamberlin,[§] and J. P. Bird[||,*]

[†]Department of Electrical Engineering, Arizona State University, Tempe, Arizona 85287-5706, United States

[‡]Micron Technology, Boise, Idaho 83716-9632, United States

[§]Department of Physics, Arizona State University, Tempe, Arizona 85287-1504, United States

[||]Department of Electrical Engineering, University at Buffalo, Buffalo, New York 14260-1920, United States

S *Supporting Information*

ABSTRACT: We demonstrate large (>100%) time-dependent magnetoresistance in nickel-silicide nanowires and develop a thermodynamic model for this behavior. The model describes nonequilibrium heating of localized spins in an increasing magnetic field. We find a strong interaction between spins but no long-range magnetic order. The spins likely come from unpaired dangling bonds in the interfacial layers of the nanowires. The model indicates that although these bonds couple weakly to a thermal bath, they dominate the nanowire resistance.
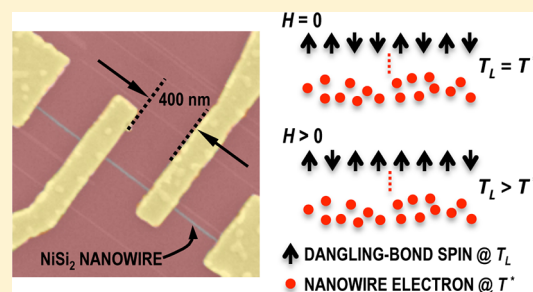
As techniques for the synthesis of nanostructured matter have advanced, there have been wide reports of unexpected magnetism in traditionally nonmagnetic materials.[1−9] While the detailed behaviors differ from one system to another, the magnetism has generally been attributed to novel chemical and/or electronic changes arising at nanostructured interfaces. One of the most widely studied interfaces is that of Si/SiO_2, whose interfacial dangling bonds (DBs) can critically influence transistor performance. It has long been known that these bonds, which may carry a net moment due to an unpaired spin, are capable of collective magnetism. Both ferromagnetic (FM) and antiferromagnetic (AFM) behavior has been reported in amorphous Si, dependent upon the degree of its disorder.[10−15] Associated characteristic temperatures (T_c, which may be a Curie/Néel temperature for FM/AFM ordering) are very low (~1 K), however, indicating that the interaction responsible for the magnetism is very weak. Similarly, AFM behavior has also been reported in amorphous Ti_xSi_{1-x} alloys, again with small T_c values ($|T_c| < 1$ K) that are consistent with a weak interaction.[16] Moreover, a recent theoretical study has predicted intrinsic antiferromagnetism at the Si(553)−Au interface, which may be a general property of miscut Si surfaces that have a graphitic step edge.[17] The predicted AFM coupling is relatively strong (15 meV ~ 170 K), but the magnitude of the interaction may be influenced by several factors, including doping. Furthermore, magnetic ordering of two-dimensional spin systems is often suppressed due to fluctuations.[18]

Transition-metal silicides are key components of modern nanoelectronics. Although normally nonmagnetic in bulk, these materials have been found to show evidence of surprising magnetic behavior when synthesized in nanowire (NW) form.[7−9] Seo et al.[7] reported magnetic hysteresis in CoSi NWs, even though this material is known to be nonmagnetic in bulk, and attributed this to uncompensated Co spins at the NW surface. Elsewhere, we have reported a pronounced low-temperature magnetoresistance (MR) in $NiSi_2$ NWs (see, for example, Figure 1a)[8,9] with an amplitude very much larger (in some cases exceeding 100%) than that exhibited by typical metals. This large MR shows strong hysteresis (such as that in Figure 1b) despite the nonmagnetic character of this material in bulk. From studies of the temperature (T) dependence of the MR, an apparent T_c of 2−5 K was inferred,[9] reminiscent of reports of weak DB magnetism in amorphous Si[10−15] and Si alloys.[16] The microscopic origins of this large MR remain unclear, but we have suggested that unpaired DBs are intimately linked to its observation.[8,9] These DBs should be abundant in the amorphous oxide layer that coats the NW core,[17] allowing them to strongly influence conduction through the metallic interior of the NW. To date, however, a convincing explanation of the time- and temperature-dependent MR has been lacking.
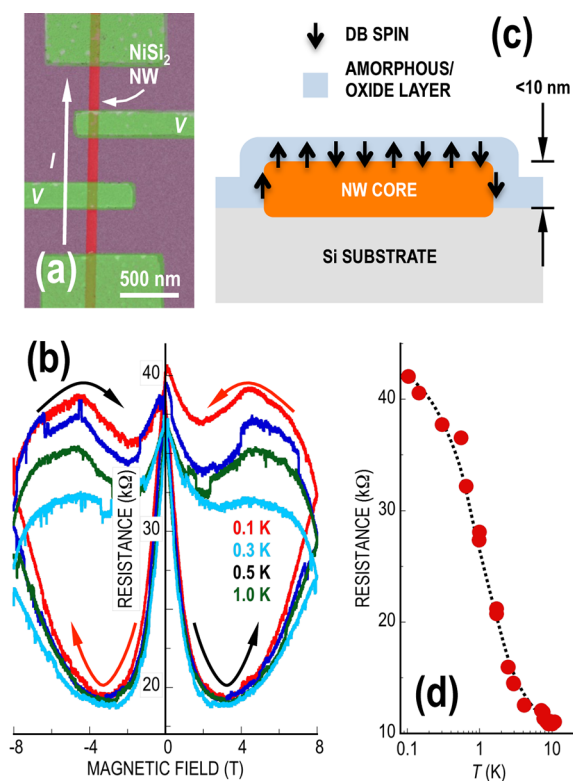
Figure 1. (a) False-color electron micrograph of the contacted NW. (b) Hysteretic MR measured at different values of T^* (indicated by legend) and for a field-sweep rate of 0.2 T/min. Arrows indicate the direction of the magnetic field sweep, starting from +8 T. (c) Schematic image illustrating the microscopic model proposed to explain the large NW MR. The schematic shows a cross section of the NW and its surrounding environment. Individual arrows in the figures denote single DB spins. (d) NW resistance as a function of the equilibrium ($H = 0$) temperature. The dotted line represents a Langevin function for classical spins (see discussion of eq 5 in main text).

A characteristic feature of nanostructures is that they are easily driven out of equilibrium, for example, by applying an electric field or by subjecting them to electromagnetic radiation. This characteristic follows from the fact that the fundamental excitations of such systems can be strongly decoupled from each other, particularly at low temperatures. It is this idea that we exploit here to explain the large MR of silicide NWs in a quantitative model that addresses heat exchange between the localized DB moments and the NW core (see Figure 1c, which represents a schematic cross section of the NW and its surrounding environment). The two key assumptions of our model are that there is weak thermal coupling between the DBs and the rest of the sample (so that significant nonequilibrium heating of the DBs may occur via adiabatic magnetization as a field is applied) and that there is a strong influence of the DB magnetic order on the resistance of the NW. New experimental results, addressing the time-dependent character of the MR, are presented to confirm the predictive capacity of this model. Our results reveal a complex interplay of interfacial magnetism and nonequilibrium energy transfer in nanostructured materials with a strong influence on the MR not found in bulk matter.

The NiSi$_2$ NWs studied here were grown on miscut Si(111) substrates by reactive epitaxy and were contacted as described in ref 19. Large MR has been found in studies of several NWs, and we focus here on a comprehensive study of one of these.

Figure 1a shows the contact configuration of this NW, and for MR measurements the magnetic field was applied perpendicular to the plane of the NW substrate. Structural characterization[19] reveals the NWs to have a crystalline core and an amorphous outer layer that is typical of most silicides. As mentioned already, this nonstoichiometric layer should serve as a source of DBs. Although NiSi$_2$ is nonmagnetic in bulk,[20] similar hysteretic MR to that which we discuss has also been found in TiSi$_2$ films,[8] so that clustering of magnetic Ni can be excluded as the source of the large MR. The sample was mounted in a dilution refrigerator, whose temperature (T) was measured in a field-compensated region by a RuO$_2$ resistor. Even at 0.1 K, the largest temperature rise in T detected during field sweeps was <25 mK. More precisely, this was the change in cryostat temperature, which should be close to that of the NW lattice. MR measurements were made by lock-in detection at ~11 Hz, using nA-level constant currents to avoid carrier heating.

The essential phenomenon that motivates this work is presented in Figure 2a, which shows the result of measuring the
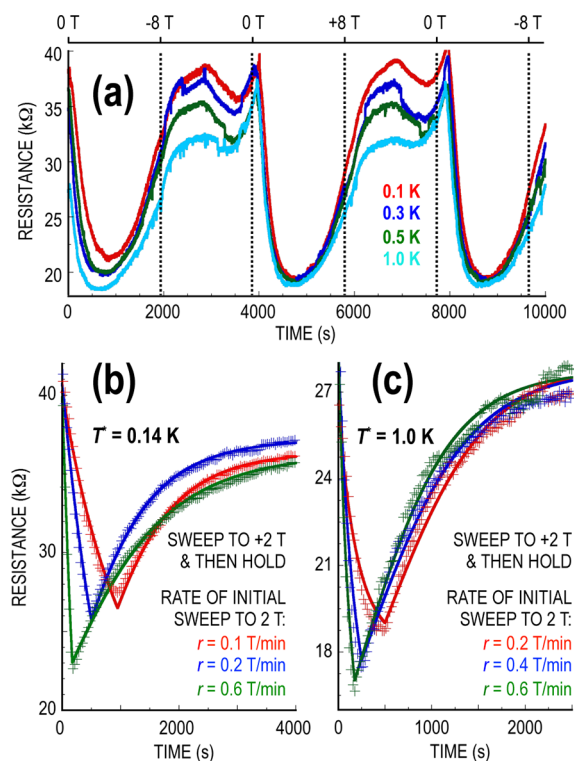

Figure 2. (a) Hysteretic MR plotted in the time domain. The upper horizontal axis denotes the magnetic field at various times during the sweep. (b,c) MR-relaxation measurements at $T^* = 0.14$ (b) and 1.0 K (c). Different curves come from sweeping the field at different rates (see legends). In each case the field is first swept from zero to +2 T, and then held at +2 T for the remainder of the measurement. Solid curves through the data represent fits performed using eqs 1−3. For fit parameters, see the Supporting Information.

change of NW resistance ($R(t)$) as the magnetic field is swept at a constant rate over a loop (from $0 \rightarrow -8 \rightarrow +8 \rightarrow 0 \rightarrow -8$ T $\rightarrow$ ...). (These data were used to construct the hysteretic MR plots of Figure 1b.) Data are plotted for several cryostat temperatures, and for the lowest-temperature data we see a MR change as large as 100%. On ramping away from zero field there is initially a rapid decrease in MR, which is then followed by a

much slower increase. These variations suggest the role of competing physical mechanisms, and motivate us to think in terms of the established ideas for adiabatic demagnetization and thermal cooling.[21,22] While these ideas usually emphasize the thermal energy removed from the surrounding environment when a spin system is demagnetized, here we also include the energy added when a spin system is magnetized. The spins in question are derived from the localized DBs, and a key assumption of our model is of a weak thermal link between these spins and the NW lattice and carriers (which are taken here to be in equilibrium with each other and characterized by a single bulk temperature, T^*). The weak link is important since it allows spins heated by an external magnetic-field to achieve a nonequilibrium local temperature (T_L) that may differ significantly from T^* over long periods of time. Indeed, our experiments suggest that full return of T_L to T^* can take more than an hour, a very long time scale that justifies the assumption of a thermally isolated DB system. A possible mechanism is that the DBs form a geometrical restriction, which may cause a weak one-dimensional link between the spins and the bulk sample. Alternatively, since the DBs couple to the rest of the sample through an interface, this may cause a mismatch in vibrational properties that yields a Kapitza-like thermal resistance.[23] Such a bottleneck has in fact been suggested previously to account for the observation of hysteresis in measurements of moderately doped semi-conductors near the metal−insulator transition.[24−26]

To quantify the weak thermal link we calculate the local temperature and its change relative to the bulk temperature: $\Delta T \equiv T_L - T^*$. For adiabatic spins, thermodynamic principles[27] predict that changes in temperature are proportional to the temperature-dependent slope of the magnetic moment $(\partial M/\partial T_L)_H$ divided by the heat capacity at constant pressure c_p

$$dT = -T \int \frac{(\partial M/\partial T_L)_H}{c_p} dH \tag{1}$$

where H is the externally applied magnetic field. Neglecting thermal expansion, the heat capacity can be written as $c_p = (\partial E/\partial T_L)$. For paramagnetic spins, the energy $E = -MH$ yields $(\partial M/\partial T_L)_H = -c_p/H$ for the numerator of the integrand in eq 1. Thus, integrating both sides of eq 1 gives

$$\Delta T = \alpha \Delta H \tag{2}$$

Here, α is a thermomagnetic coupling coefficient that comes from the constant of integration and which depends on the relative starting points of the temperature and field. The experimental data (see below) yield a typical temperature increase per unit field change of $\alpha \sim 0.5$ K/T.

For simplicity we assume a single time constant τ for the thermal coupling between the spin system and phonon bath. This τ is assumed to depend only on the sample temperature T^*, not on the local DB temperature. The difference, ΔT, is usually positive as the spins are magnetized (adiabatic magnetization) but may become negative as the spins are demagnetized, eventually returning to zero with time-constant τ. As noted already, we find very weak thermal coupling ($\tau > 200$ s), indicating that ΔT may exceed 1 K for several minutes. Time-dependent changes in temperature are given by Newton's law of cooling, modified to include α from eq 2

$$\frac{d\Delta T}{dt} = -\frac{\Delta T}{\tau} + \alpha \frac{dH}{dt} \tag{3}$$

For the measurements presented here, the field is changed by sweeping linearly at a constant rate (i.e., $dH/dt = r$, where r is a constant with units of T/s). Equation 3 can be solved in two time regimes, (a) while the field is changing from its initial value to its final value, $0 \rightarrow t_{fin}$, and (b) while the field is held constant at its final value, yielding

$$\Delta T = \alpha r \tau (1 - e^{-t/\tau}) \quad t \leq t_{fin} \tag{4a}$$

$$\Delta T = \alpha r \tau (e^{t_{fin}/\tau} - 1)e^{-t/\tau} \quad t \geq t_{fin} \tag{4b}$$

We compare the behavior predicted by eq 4 with measurements of the time-dependent change in NW resistance, observed in response to a variation of the magnetic field. In the first set of measurements, shown in Figure 2b,c, the field is swept from zero to 2 T (where the MR hysteresis is maximal), then held at 2 T for about an hour. Figure 2b shows measurements obtained at a sample temperature of $T^* = 0.14$ K, while Figure 2c shows similar measurements at $T^* = 1.0$ K. The initial decrease of resistance seen in all curves is obtained while sweeping from zero to 2 T with the subsequent increase observed while holding the field fixed at 2 T. The three different curves at each temperature correspond to different field-sweep rates, r, with the largest initial reduction in resistance being observed for the fastest sweep rate. This is consistent with expectations, since the relaxation term in eq 3 ($-\Delta T/\tau$) has less time to act for this rate. Qualitatively, the reduction in resistance is due to local heating of the DBs as the spins are adiabatically magnetized, while the subsequent slow relaxation occurs as excess heat flows slowly from the DBs to the bulk thermal bath of the NW. Quantitatively, the connection between local temperature and NW resistance is made using the measured equilibrium ($H = 0$) temperature dependence (see Figure 1d). We find that the NW resistance is well described by the Langevin function for classical spins

$$R = R_0 + A\left[\coth\left(\frac{b}{T}\right) - \frac{T}{b}\right] \tag{5}$$

Here R_0 is a residual resistance at high temperatures (where the magnetic order goes to zero), A is an amplitude factor that comes from the coupling between the magnetization and the NW resistance, and b is the characteristic temperature of the Langevin function. From the data shown in Figure 1d, we obtain experimental values: $R_0 = 8.0 \pm 0.4$ kΩ, $A = 36.0 \pm 0.8$ kΩ, and $b = 1.95 \pm 0.12$ K, yielding the dotted line through the data. Theoretically, a magnetic moment of one Bohr magneton per spin is expected for Si atoms at a Si(553)−Au surface step.[17] With this assumption, $b = 0.672$ (K/T) H_{loc}, where H_{loc} is the local field at each spin. The measured b found from the NW resistance in zero-applied field indicates a local field of $H_{loc} \approx 3$ T. Such a large local field suggests a strong interaction between spins. The lack of any clear magnetic transition may be due to thermal fluctuations that prohibit magnetic order for isotropic spins in 2D,[18] consistent with the Langevin function used to describe the temperature-dependent resistance.

We characterize the measured time-dependent MR of the NW using the change in local temperature from eq 4, converted to resistance using eq 5. The field sweep rate (r), final time of the sweep (t_{fin}), and sample temperature (T^*) are fixed by the experiment. We also fix the resistance parameters $R_0 = 8.0$ kΩ and $A = 36.0$ kΩ from the measured temperature dependence, leaving α, τ, and b as adjustable parameters. Note that from all the time-dependent measurements we find $b = 1.74 \pm 0.36$ K

(see Supporting Information), within experimental error of the value determined above from the Langevin temperature dependence. A fourth adjustable parameter R_{fin} from the static MR described in ref 9 is simply added to eq 5 during the field-ramp process: $R_0 \rightarrow R_0 + R_{fin}t/t_{fin}$ for $t \leq t_{fin}$, and $R_0 \rightarrow R_0 + R_{fin}$ for $t \geq t_{fin}$. We use a Levenberg−Marquardt nonlinear least-squares-fit procedure with eq 4 inserted into eq 5 and adjust the parameters to obtain best overall agreement with the measured resistance as a function of time. Results are shown in Figures 2b,c. The overall quality of the fits is quite good and the tables in the Supporting Information show that the time constant and thermomagnetic coefficient (τ and α) have no systematic dependence on the rate of field change at each temperature. However, as a function of temperature, α increases with increasing temperature, while at 1.0 K τ has decreased to 50% of its low-temperature value. Continuing this decrease in τ, the hysteresis in the MR would be too fast to measure at temperatures much above 3 K.

Another test of the model is shown in Figure 3. Here, the field is first swept from zero to 2 T, as before. Again the field is
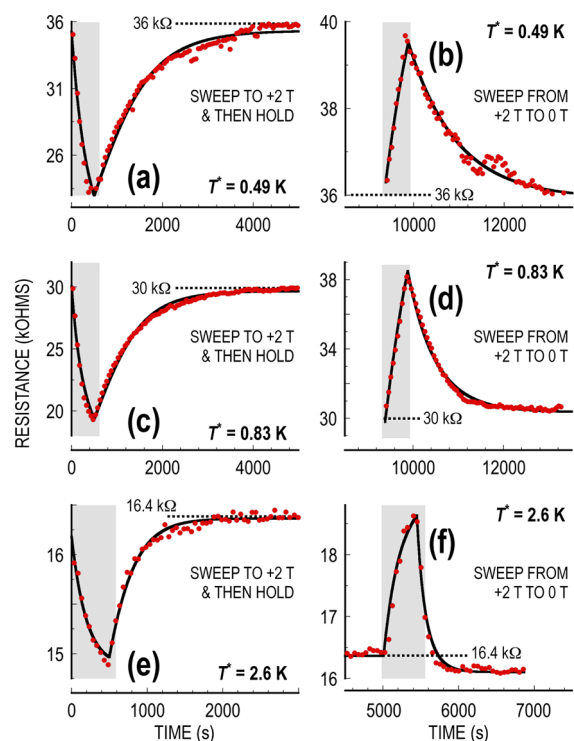

Figure 3. Two-stage MR-relaxation measurements. Panels (a,c,e) were obtained by sweeping the field from zero to +2 T and then holding at +2 T. Subsequently, panels (b,d,f) were obtained after allowing the sample to equilibrate for a long time (as indicated by the offset in the time axis), before sweeping the field down from +2 T to zero. In each of the panels, the gray region denotes the interval over which the magnetic field was swept. Field sweep rates are 0.2 T/min in each of the panels and the temperature (T^*) is indicated. Solid curves through the data represent fits performed with eqs 1−3. Fit parameters for all three experiments are provided in the Supporting Information.

held at 2 T, but for a longer time until the sample has fully equilibrated (Figure 3a,c,e). Finally the field is swept back down to zero, yielding an initial rise in resistance as shown in Figure 3b,d,f. Qualitatively, the rise in resistance is due to adiabatic demagnetization that cools the DBs. As before, there is a subsequent slow relaxation, but now the resistance relaxes

downward as heat flows slowly into the DBs from the sample, raising the DB temperature. Equation 3 can also be used to characterize this behavior. Although we achieve optimized fitting by adjusting the value of the thermomagnetic coupling coefficient, there is no systematic difference between ramping the field up or down. Thus, the clear difference in amplitude of the downward and upward resistance peaks shown in the various panels of Figure 3 can be attributed to the difference in the temperature-dependent slopes of the resistance from the Langevin function above and below each measurement temperature. Figure 3e,f shows the same field ramp up to 2 T and back down but at a higher temperature, $T^* = 2.6$ K. The agreement with eq 3 is again quite accurate. Note, however, that the long-time baseline now shows a significant positive MR. This static MR may be due to weak antilocalization.[19]

The model we have developed can be interpreted as follows. As the magnetic field is increased, the DB spin-wave excitations are reduced, thereby reducing the magnon entropy. The reduced magnon entropy is converted to increased DB phonon entropy (local heating), which due to the weak thermal link between the DBs and the NW lattice causes an increase in the local temperature of the spins (T_L) and a decrease in the NW resistance. The measured resistance as a function of temperature allows us to attribute the MR to isotopic spins in a large local field. The local field may come from the exchange interaction between spins, while the increased entropy from strong fluctuations of the two-dimensional isotropic spins, predicted by the Mermin-Wagner theorem, prevents magnetic ordering down to very low temperatures. Although the thermal contact between the localized DBs and the bulk NW is very weak, the magnetic order of the DB spins strongly influences the electrical properties of the NW, causing a large change in resistance with changing temperature and large MR with changing magnetic field. Using these ideas we have shown that it is possible to achieve a quantitative description of several features of our data. For example, referring to Figure 1b, there is a large asymmetry in the MR as the field crosses zero. The model combines adiabatic demagnetization that cools the spins when the magnitude of the magnetic field decreases with adiabatic magnetization that heats the spins when the magnetic field increases. These processes usually exhibit asymmetry, especially at low temperatures where the Langevin function is already nearly saturated.

In conclusion, we have developed a model for the large MR of silicide NWs that is based on the concept of nonequilibrium heating of localized spins. Using the measured variation of the NW resistance as an effective thermometer for these spins, we are able to reliably reproduce the MR transients obtained under different field-sweep conditions and at different temperatures. The key assumptions of our model are of a weak thermal link between the localized spins and the other components of the NW and a strong influence of the magnetic order on the resistance of the NW. As such, the model indicates that although spins couple weakly to a thermal bath, they dominate the nanowire resistance.

■ ASSOCIATED CONTENT

Ⓢ Supporting Information

Consists of tables that list the values of the parameters used to fit the experimental data in Figures 2 and 3. This material is available free of charge via the Internet at http://pubs.acs.org.

■ AUTHOR INFORMATION

Corresponding Author
*E-mail: jbird@buffalo.edu. Phone: +1 (716) 645-1015.

Author Contributions
The authors contributed equally to this work.

Notes
The authors declare no competing financial interest.

■ REFERENCES

(1) Brinkman, A.; Huijben, M.; Zalk, M. V.; Huijben, J.; Zeitler, U.; Maan, J. C.; van der Wiel, W. G.; Rijnders, G.; Blank, D. H. A.; Hilgenkamp, H. *Nat. Mater.* **2007**, *6*, 493−496.

(2) Zhong, Z.; Kelly, P. J. *Europhys. Lett.* **2008**, *84*, 27001.

(3) Rogachev, A.; Wei, T.-C.; Pekker, D.; Bollinger, A. T.; Goldbart, P. M.; Bezryadin, A. *Phys. Rev. Lett.* **2006**, *97*, 137001.

(4) Wei, T.-C.; Pekker, D.; Rogachev, A.; Bezryadin, A.; Goldbart, P. M. *Europhys. Lett.* **2006**, *75*, 9432006.

(5) Qiu, X.; Li, L.; Tang, C.; Li, G. *J. Am. Chem. Soc.* **2007**, *129*, 11908−11909.

(6) Deng, S.; Loh, K. P.; Yi, J. B.; Ding, J.; Tan, H. R.; Lin, M.; Foo, Y. L.; Zheng, M.; Sow, C. H. *Appl. Phys. Lett.* **2008**, *93*, 103111.

(7) Seo, K.; Varadwaj, K. S. K.; Mohanty, P.; Lee, S.; Jo, Y.; Jung, M.-H.; Kim, J.; Kim, B. *Nano Lett.* **2007**, *7*, 1240−1245.

(8) Kim, T.; Naser, B.; Chamberlin, R. V.; Schilfgaarde, M. V.; Bennett, P. A.; Bird, J. P. *Phys. Rev. B* **2007**, *76*, 184404.

(9) Kim, T.; Chamberlin, R. V.; Bennett, P. A.; Bird, J. P. *Nanotechnology* **2009**, *20*, 135401 (2009).

(10) Brodsky, M. H.; Title, R. S. *Phys. Rev. Lett.* **1969**, *23*, 581−585.

(11) Hudgens, S. J. *Phys. Rev. B.* **1976**, *14*, 1547−1556.

(12) Disalvo, F. J.; Bagley, B. J.; Hutton, R. S.; Clark, A. H. *Solid State Commun.* **1976**, *19*, 97−100.

(13) Thomas, P. A.; Brodsky, M. H.; Kaplan, D.; Lepine, D. *Phys. Rev. B.* **1978**, *18*, 3059−3073.

(14) Askew, T. R.; Stapleton, H. J.; Brower, K. L. *Phys. Rev. B.* **1986**, *33*, 4455−4463.

(15) Khokhlov, A. F.; Mashin, A. I.; Satanin, A. M. *Phys. Status Solidi B* **1981**, *105*, 129−136.

(16) Rogatchev, A. Yu.; Mizutani, U. *J. Phys.: Condens. Matter* **2000**, *12*, 4837−4849.

(17) Erwin, S. C.; Himpsel, F. J. *Nat. Comm.* **2010**, *1*, 58.

(18) Mermin, N. D.; Wagner, H. *Phys. Rev. Lett.* **1966**, *17*, 1133−1136.

(19) Lin, J.-F.; Bird, J. P.; He, Z.; Bennett, P. A.; Smith, D. J. *Appl. Phys. Lett.* **2004**, *85*, 281−283.

(20) Nava, F.; Tu, K. N.; Mazzega, E.; Michelini, M.; Queirolo, G. *J. Appl. Phys.* **1987**, *61*, 1085−1093.

(21) de Haas, W. J. *Nature* **1933**, *132*, 372−373.

(22) Tegus, O.; Brück, E.; Buschow, K. H. J.; de Boer, F. R. *Nature* **2002**, *415*, 150.

(23) Norris, P. M.; Hopkins, P. E. *J. Heat Transfer.* **2009**, *131*, 043207.

(24) Andreev, A. G.; Chernyaev, A. V.; Egorov, S. V.; Parfeniev, R. V.; Zabrodskii, A. G. *Phys. Status Solidi B* **2000**, *218*, 165−168.

(25) Egorov, S. V.; Zabrodskii, A. G.; Parfen'ev, R. V. *Semiconductors.* **2004**, *38*, 192−196.

(26) Zabrodskii, A. G. *Phys. Status Solidi B* **2004**, *241*, 33−39.

(27) Kunzler, J. E.; Walker, L. R.; Galt, J. K. *Phys. Rev.* **1960**, *119*, 1609−1614.